HHS Public Access

Author manuscript

Proteomics. Author manuscript; available in PMC 2019 August 07.

Published in final edited form as:

Proteomics. 2019 February ; 19(4): e1800353. doi:10.1002/pmic.201800353.

UCP2 overexpression redirects glucose into anabolic metabolic pathways

Annapoorna Sreedhar[1], **Teresa Cassell**[2], **Parker Smith**[1], **Daiwei Lu**[1], **Hyung W. Nam**[1], **Andrew N. Lane**[2,*], **Yunfeng Zhao**[1,*]

[1]Department of Pharmacology, Toxicology & Neuroscience, LSU Health Sciences Center, Shreveport, LA 71130;

[2]Department of Toxicology and Cancer Biology, University of Kentucky College of Medicine, Lexington, KY 40509

Abstract

Uncoupling protein 2 (UCP2) is often upregulated in cancer cells. The UCP2 upregulation is positively correlated with enhanced proliferation, tumorigenesis, and metabolic alterations, thus suggesting that UCP2 upregulation could play a key role in sensing metabolic changes to promote tumorigenesis. To determine the global metabolic impact of UCP2 upregulation, we used $^{13}C_6$ glucose as a source molecule to 'trace' the metabolic fate of carbon atoms derived from glucose. UCP2 overexpression in skin epidermal cells enhanced the incorporation of ^{13}C-label to pyruvate, TCA cycle intermediates, nucleotides, and amino acids, suggesting that UCP2 upregulation reprograms cellular metabolism towards macromolecule synthesis. To the best of our knowledge, this is the first study to bring to light the overall metabolic differences caused by UCP2 upregulation.

Keywords

Uncoupling protein 2; tumorigenesis; metabolomics; metabolite profiling; mitochondrial metabolism; bioenergetics

INTRODUCTION

In recent times, much attention has been paid to the altered metabolism and metabolic reprogramming in cancer cells [1]. Cancer cells reprogram their metabolism to withstand the increased metabolic demands of cell growth and proliferation. A long-established example of reprogrammed metabolism in cancer cells is the Warburg effect, in which cancer cells heavily depend on lactic fermentation for energy production even in the presence of oxygen [2, 3]. Warburg later proposed that the damaged mitochondria are the primary reason for the

*To whom correspondence should be addressed: Yunfeng Zhao, Ph.D., Department of Pharmacology, LSU Health Sciences Center, Shreveport, LA 71130, yzhao1@lsuhsc.edu; Tel: (318) 675-7876; Fax: (318) 675-7857., Andrew N. Lane, Center for Environmental and Systems Biochemistry, University of Kentucky, Lexington, KY 40506, andrew.lane@uky.edu; Tel: (859) 218-2868.

Author contributions: ANL and YZ designed the experiments. AS, TC, and PS performed the experiments. AS, TC, PS, HWN, ANL, and YZ analyzed the data. AS, ANL, and YZ wrote the manuscript.

Conflict of interest: The authors declare no conflict of interest with the contents of this article.

effect and thence cancer initiation [4], though more recent data show that mitochondria are typically very active in respiration and the Krebs cycle, but may oxidize fuels other than glucose [5–7]. Indeed, numerous studies show that cancer cells *in vitro* and *in vivo* can utilize a variety of substrates depending on the genetic lesion of the tumor and the microenvironment [8–13], and reprogrammed metabolism is considered as one of the major hallmarks of cancer cells [1].

Although the Warburg's theory of cancer cells has been challenged by later findings [14, 15], mitochondrial metabolic alterations are important contributors to metabolic reprogramming of cancer cells. Mitochondria play crucial roles in tumor cell initiation, progression, differentiation, and metabolism [16]. Numerous mitochondrial defects and/or alterations have been suspected to contribute to the pathogenesis and progression of cancer [17, 18]. One such mitochondrial alteration leading to tumor promotion is the amplification of the gene expression for mitochondrial uncoupling protein 2 (UCP2) [19, 20]. UCP2 is an anion transporter present in the inner mitochondrial membrane, whose physiological role is to decrease the mitochondrial membrane potential and reactive oxygen species (ROS) production [21, 22]. We have previously demonstrated that UCP2 is overexpressing at the protein level in several human cancers [23]. The increased levels of UCP2 have been linked to enhanced cell proliferation and tumorigenicity [20, 24]. Furthermore, our results showed that UCP2 overexpression promoted skin tumorigenesis via altering glucose and lipid metabolism, and the key regulators of metabolic processes [25, 26]. As such, UCP2 is thought to be a crucial player in the cascade of molecular and metabolic events associated with carcinogenesis. Although it remains unclear exactly how UCP2 elevation exerts its pro-tumorigenic effect at the molecular level, a growing body of evidence suggests that UCP2 plays an important role in tumor cell metabolic reprogramming [27]. Additionally, UCP2 has been speculated to act as a "metabolic switch" coupling glucose oxidation to mitochondrial metabolism [28].

However, to date, very little is known regarding the global metabolic impact of UCP2 overexpression in cancer. Thus, questions arise as to the major metabolic differences between a normal cell and one overexpressing UCP2. Therefore, to decipher the influence of UCP2 overexpression on cellular metabolism, we performed overall pathway analysis using the stable-isotope resolved metabolomics (SIRM) approach [29]. UCP2 overexpressing cells were generated by transfecting JB6 P+ cells with a human UCP2-containing vector or an empty base vector (pCMV6) as described previously [25, 26]. UCP2 overexpressing and control pCMV cells were labeled with uniformly ^{13}C-enriched glucose to 'trace' the fate of carbon atoms derived from ^{13}C-glucose. Thus, the use of $^{13}C_6$ glucose allowed identification of major differences in glucose utilization between UCP2 overexpressing and control pCMV cells.

To the best of our knowledge, this is the first study of its kind to provide direct evidence for the existence of metabolic alterations caused by UCP2 overexpression, therefore, establishing it as an important metabolic target for a potential therapy.

Materials and methods

Cell lines and treatments

Murine skin epidermal cells (purchased from American Type Culture Collection, Manassas, VA) are the only well-characterized skin cell model to study tumor promotion [30]. Stable UCP2 overexpressing and control pCMV cells were generated as previously described [25, 26]. Briefly, JB6 P+ (CL-41) cells were transfected with a human UCP2-containing or an empty pCMV6 vectors (purchased from OriGene, Rockville, MD. Catalog number SC320879, and PS100001, respectively) and stable clones were established.

Tracer treatment and metabolomics analysis

Cells were cultured in 10-cm culture dishes (purchased from Thermo Fisher Scientific, Waltham, MA) to approximately 70% confluent in MEM media (purchased from Corning, Corning, NY), supplemented with 4% FBS, 1x streptomycin-penicillin, and 2 mM L-glutamine. On the day of the treatment, old media were removed and replaced with glucose-free MEM media (purchased from Corning) containing 2 mM $^{13}C_6$-glucose (purchased from Cambridge Isotope Laboratories, Tewksbury, MA). Medium was collected at 0 and 24 h to determine the rates of glucose uptake, lactate alanine/glutamate excretion, and the fraction of glucose that was converted to lactate. After 24 h of incubation, media were removed, plates were washed with cold PBS to remove media components, and cells were harvested and collected for metabolomics analysis as described below.

Sample preparation

SIRM studies were carried out as previously described [5, 29]. The cells were rinsed three times with ice-cold PBS. Cells were lyzed and metabolism was quenched on the plate using 2 mL cold CH_3CN, 1.3 mL nanopure water and 0.2 ml 0.2 mM Tris-HCl pH 8.0. One ml of chloroform was added to the quenched cells, making a final 2:1.5:1 CH_3CN to water to chloroform ratio, and samples were shaken vigorously. The extraction mixture was centrifuged at 3,500 x g for 20 min at 4 °C to yield polar (top layer) and non-polar (bottom layer) metabolites. The extraction was performed again using 2:1:1mM chloroform: methanol: BHT (butylated hydroxytoluene) for quantitative recovery. Solvents were then removed from the polar extracts by lyophilization following distribution for separate analyses.

NMR Analysis

NMR spectra were recorded at 14.1-T on an Agilent DD2 spectrometer with automation in 1.7-mm tubes in a 3-mm inverse HCN cold probe at 15 °C. Samples reconstituted in D_2O were maintained at 6 °C prior to NMR analysis. ^1H PRESAT spectra were recorded with 512 transients an acquisition time of 2 sec over a spectral width of 10 ppm and a presaturation delay of 4 s, using a weak transmitter rf field for saturating the strong solvent signal (52 min.). 1D $^1H\{^{13}C\}$ HSQC spectra were recorded with 1024 transients over a spectral width of 10 ppm were recorded with an acquisition time of 0.2 s and a recycle time of 2 s with GARP decoupling during the acquisition time (34.5 min). Compounds were identified from chemical shifts and splitting patterns, cross-referenced to 2D spectra, using our in-house

database [31] and those of HMDB [32]. We used a targeted analysis for a small number of abundant compounds as per protocol for non-SIRM experiments. Where possible, we also estimated the ^{13}C enrichment at individual positions such as lactate and Ala methyl groups and glucose H1 from the ^{13}C satellites in ^{1}H NMR spectra as well as from the 1D HSQC spectra as described previously [29]. Data were analyzed using MNova v 10.0 (Mestrelab Research, Santiago de Compostela, Spain). Free induction decays were linear predicted once and zero filled and apodized using an unshifted Gaussian peak and a line broadening exponential (1 Hz for PRESAT and 4 Hz for HSQC). Spectra were phased, baseline corrected with a simple third order polynomial, and referenced to DSS, Concentrations were determined by peak integration with normalization to the DSS resonance at 0 ppm, with corrections for partial saturation as described [31].

IC-FTMS

Ion chromatography- Fourier transform-MS was performed as previously described [33]. Briefly, polar extracts were reconstituted in 20 μL nanopure water, and analyzed by a Dionex ICS-5000+ ion chromatograph interfaced to an Orbitrap Fusion Tribrid mass spectrometer (Thermo Fisher Scientific, San Jose, CA, USA) operating at a resolution setting of 500,000 (FWHM at *m/z* 200) on MS1 acquisition to capture all ^{13}C isotopologues. The chromatography was performed using a Dionex IonPac AG11-HC-4 μm RFIC&HPIC (2 × 50 mm) guard column upstream of a Dionex IonPac AS11-HC-4 μm RFIC&HPIC (2 × 250 mm) column. Chromatography and mass spectrometric settings were the same as described previously [31] with an acquisition *m/z* range of 80 to 700. Metabolites and their isotopologues were identified by chromatographic retention times and their *m/z* values compared with those of the standards. Peak were integrated and the areas exported to Excel via the TraceFinder 3.3 (Thermo, Waltham, MA, USA) software package. Peak areas were corrected for natural abundance as previously described [34], after which fractional enrichment and μmoles metabolites/g protein were calculated to quantify ^{13}C incorporation into various metabolites.

Statistical analysis

Statistical software SAS 9.4 (SAS Institute Inc, Cary, NC) was used for data analysis. Two-way ANOVA was used followed by the Bonferroni post hoc test for multiple comparisons. Data were reported as means ± standard error (S.E.M.). $p<0.05$ was considered significant.

Results and Discussion

The dual metabolic nature of UCP2 overexpressing cells

We grew JB6 P+ (CL-41) cells, murine skin epidermal cells with and without overexpression of UCP2 in the presence of $^{13}C_6$ glucose for 24 h and measured both intracellular and extracellular metabolite levels and isotopomer distributions as described in the Methods section.

The amounts of glucose taken up and lactate excreted into the culture media were measured by ^{1}H-NMR as described previously [33, 35–36]. We used both 1D ^{1}H NMR and 1D ^{1}H-{^{13}C}-HSQC (Figure S1) which enables a direct comparison of changes in ^{13}C enrichment

at specific positions of metabolites between control (pCMV) and UCP2 overexpressing cells [37]. As shown in Fig. 1a, the consumption of $^{13}C_6$-glucose by UCP2 overexpressing cells was slightly decreased (approximately 18%) compared to the consumption by control pCMV cells. At the same time the amount of [$^{13}C_6$] lactate excreted into the media was significantly decreased (approximately 51%) in UCP2 overexpressing cells, and essentially all of the lactate derived from exogenous glucose (Fig. 1b). The concentration of ^{13}C-lactate in the cell extract, corresponding to intracellular lactate, was significantly enhanced in UCP2 overexpressing cells Fig. 1c).

We are also intrigued by this apparent decrease in the ratio of glucose consumption and lactate secretion in UCP2 overexpressing cells, however, it has been demonstrated that under conditions such as lactic acidosis, certain cancer cells become less glycolytic and more oxidative [37]. Hence, it is interesting to speculate that the reduction in the rate of glucose consumption and net lactate generation in UCP2 overexpressing cells may be a result of lactic acidosis. A possible explanation is that UCP2 overexpressing cells were initially glycolytic [26], then, due to increased accumulation of lactate and acidification of medium, may have resulted in a corresponding decrease of glucose consumption and lactate generation. Nevertheless, further investigations are necessary to evaluate whether lactic acidosis is the cause of transition from the Warburg effect to a nonglycolytic mode observed in UCP2 overexpressing cells.

UCP2 overexpression increases ^{13}C labeling in pyruvate

Since the production of intracellular lactate accounted for a relatively small part of the glucose consumed, we traced the carbon flow from $^{13}C_6$-glucose through glycolysis. The metabolism of glucose through glycolysis generates pyruvate as the end product, which under aerobic conditions can be converted to several compounds other than lactate, including alanine, OAA and acetyl coenzyme A, the latter enters the TCA cycle (Figures S2 and S3). As shown in Fig. 2a, the presence of $^{13}C_6$-glucose significantly increased the amount of ^{13}C enrichment of pyruvate. It is clear that UCP2 overexpressing cells had a much higher level of m+3 isotopologues of pyruvate compared to control pCMV cells. Thus, the high degree of pyruvate labeling in UCP2 overexpressing cells suggests that the major source of carbon in pyruvate was indeed glucose. Overall, these data show that a substantial amount of glucose taken up by UCP2 overexpressing cells is catabolized to pyruvate, in agreement with the lactate data shown above.

UCP2 overexpression increases pyruvate oxidation and TCA cycle flux

The decrease in lactate levels and the increase in the pyruvate levels indicate that UCP2 overexpressing cells may divert a greater percentage of carbons towards the TCA cycle. A growing body of evidence now indicates that cancer cells transport a significant portion of glucose-derived pyruvate into mitochondria where it is used for replenishing TCA cycle intermediates [10, 11]. Hence, to monitor whether UCP2 overexpressing cells utilize $^{13}C_6$-glucose as the mitochondrial anaplerotic substrate, we examined the ^{13}C labeling of various TCA cycle metabolites as summarized in Figure S3.

Most of the intermediates of the TCA cycle were ^{13}C-enriched in the UCP2 overexpressing cells, indicating that the TCA cycle metabolites derived at least in part from ^{13}C-labeled glucose. ^{13}C-labeled isotopologues of citrate (m+2, m+4) (Fig. 2b) and cis-aconitate (m+2, m+4) (Fig. 2c) were significantly higher in UCP2 overexpressing cells. In addition, UCP2 overexpressing cells exhibited enhanced levels of ^{13}C glucose-derived alpha-ketoglutarate (α-KG) (Fig. 3a), succinate (Fig. 3b), fumarate (Fig. 3c), and malate (Fig. 3d), suggesting a more highly active Krebs cycle in the UCP2 overexpressing cells. Although these results do not necessarily reflect the rate of TCA cycle operation in UCP2 overexpressing cells, nevertheless, the de novo production of these metabolites indicates that the mitochondria may not be dysregulated, and that the Krebs cycle is operative in UCP2 overexpressing cells. The succinate/fumarate and malate pools are much smaller than the citrate pool, yet are much less enriched. This implies either the carbon is syphoned off at isocitrate/α-KG, or there is another carbon source input into the TCA. This could be tested in a ^{13}C-Gln experiment for example in future studies.

Overexpression of UCP2 increases de novo amino acid synthesis

In addition to glucose, highly proliferating tumor cells have increased demand for amino acids which are critical substrates both for mitochondrial metabolism and synthesis of proteins. Intermediates in the TCA cycle provide precursors for the synthesis of several amino acids: aspartate, glutamate, and alanine can be made by transamination of oxaloacetate, α-KG, and pyruvate, respectively (cf Figs S2 and S3). Hence, amino acid production is highly dependent on TCA cycle activity. Therefore, we hypothesized that the increased Krebs' cycle activity might be responsible for greater amino acid synthesis in UCP2 overexpressing cells. As shown in Fig. 4a, the amount of ^{13}C-alanine secreted into the medium was higher in UCP2 overexpressing cells than in control pMCV cells. Pyruvate is transaminated to form alanine by alanine amino transferase (ALT). Thus, the ^{13}C-labeling in alanine shows that ALT must be active in UCP2 overexpressing cells (cf. Fig. S2). Similarly, aspartate (Asp) can be synthesized by transamination of oxaloacetic acid (OAA) via glutamic-oxaloacetic transaminase (GOT1,2) (Fig. S3). There are two major mitochondrial routes to OAA from pyruvate, either through the forward reactions of the Krebs cycle, initially generating doubly labeled OAA (and Aspartate) or via carboxylation of pyruvate via pyruvate carboxylase, generating triply labeled OAA and Asp from $^{13}C_6$-glucose (Fig. S3) [38]. As shown in Fig. 4b, although the total Asp concentration is higher in the UCP2 cells, the much higher levels of m+0 aspartate cells suggests that ^{13}C-glucose is not the major carbon source for the synthesis of aspartate.

Glutamate (Glu) can be synthesized either by the reductive amination of α-KG or by transamination with a number of amino acids. Glutamate is also the immediate precursor of glutamine (Gln). In addition, Glu is essential for glutathione (GSH) synthesis (Fig S3). We found by IC-MS that the m+2 Glu was higher in UCP2-overexpressing cells, suggesting that Glu labeling was derived from (m+2) α-KG (Fig. 4c). However, the total enrichment was far lower than in citrate, suggesting that only a small quantity glutamate derived from glucose/α-KG. In addition, there was a net excretion of ^{13}C-labeled Glu into the medium (Fig. 4d). A large fraction of Glu was present in the media in UCP2 overexpressing cells which may reflect the exchange of intracellular Glu for cystine, a major determinant of glutathione

(GSH) synthesis [39]. Accordingly, UCP2 overexpressing cells showed much more active GSH synthesis than control pCMV cells (Fig. 4e). The extent of m+2 and m+4 GSH labeling was much greater in UCP2 overexpressing cells than in the control, suggesting that the GSH was labeled with Glu residue, which was corroborated in the 1D HSQC spectra showing ^{13}C enrichment at the Glu C4 position of GSH (data not shown). Taken together, these results suggest that, UCP2 overexpressing cells demonstrate an increased *de novo* amino acid and GSH synthesis, as shown in Figure S3.

UCP2 overexpression shows significant enrichment of de novo nucleotide synthesis

In addition to amino acids, nucleotide synthesis is highly dependent on the mitochondrial metabolism. Although the synthesis of the ribose subunit is entirely cytoplasmic, pyrimidine bases are derived directly or indirectly from mitochondrial intermediates, and one step (DHODH) that is exclusively mitochondrial, which is coupled to respiration at complex II [5] (Figure S4). Since UCP2 overexpressing cells have an enhanced activity of the Krebs' cycle, it would not be surprising to find a high rate of synthesis nucleotides. Therefore, we analyzed the SIRM data to assess the fate of glucose-derived ^{13}C into purine and pyrimidine nucleotides. As shown in Fig. 5a, inosine monophosphate (IMP), the common intermediate in the purine biosynthetic pathway, was significantly enriched in UCP2 overexpressing cells. Thus, an increased m+7, m+8, and m+9 labeling of purine intermediates implies a higher rate of synthesis of purine rings building on a fully labeled phosphoribosyl pyrophosphate (PRPP) (Fig. 5b). Thus these cells are very actively synthesizing nucleotides, using both the pentose phosphate pathway and the purine pathway (cf Fig. S4). It is clear that UCP2 overexpressing cells had a much higher content of (m+6, m+7, m+8, m+9) AMP, ADP, ATP (Fig. 5c, similar trends were found and only the ATP data was shown), GMP, GDP, and GTP (Fig. 5d, similar trends were found and only the ATP data was shown), which corresponds to enhanced *de novo* purine synthesis. These higher isotopologues of the purine nucleotides indicate incorporation of glucose-derived carbon not only into the ribose subunit but also up to four of the purine base. These derive in part from glycine, which can be made via the glycolytic 3PGA through serine to glycine using SHMT1,2. Additional carbons may derive ultimately from glycine via methylene tetrahydrofolate, which may include a mitochondrial step [5–8].

For the pyrimidines, we found elevated isotopologues m+5, m+6, m+7 of UMP, UDP, and UTP (Fig. 6a) and (m+5) CMP, CDP, and CTP (Fig. 6b) in UCP2 overexpressing cells compared to control pCMV cells, indicating de novo synthesis of UMP and CMP. However the labeling of pyrimidine intermediates was less intense compared to the labeling of purine intermediates, suggesting that the $^{13}C_6$-glucose may not be the major source of carbon for uracil synthesis in UCP2 overexpressing cells, which is consistent with the low glucose-derived labeling of Asp, which is the immediate precursor to uracil synthesis. This may indicate that pyrimidine intermediates in UCP2 overexpressing cells utilize Gln rather than Glc as their main carbon source.

These data suggest that UCP2 overexpressing cells exhibit an increased *de novo* synthesis of nucleotides. The increased nucleotide synthesis in UCP2 overexpressing cells may be required for DNA synthesis and RNA production to support protein synthesis during S-

phase. Notably, we have previously demonstrated that UCP2 overexpressing cells enhanced cell proliferation by increasing the percentage of cells in the S-phase of the cell cycle. Therefore, UCP2 overexpressing cells may heavily stimulate the nucleotide biosynthesis to support their rapid proliferation as they progress through the cell cycle.

Concluding remarks

In conclusion, UCP2 overexpressing cells upregulate both energy metabolism and biosynthesis pathways. The regulation of energy and metabolic pathways is needed for nucleotide biosynthesis in highly proliferating UCP2 overexpressing cells. The ^{13}C-labeling pattern shows that the major metabolic differences between a normal cell and one overexpressing UCP2 is the increased incorporation of ^{13}C labeling into pyruvate, leading to an enhanced pyruvate oxidation and a greater TCA cycle flux in UCP2 overexpressing cells. In addition, UCP2 overexpression significantly enhances amino acid and nucleotide biosynthesis. Taken together, our data reveal that overexpression of UCP2 affects central pathways of metabolism.

Supplementary Material

Refer to Web version on PubMed Central for supplementary material.

Acknowledgements

This work was supported in part by a pilot grant from 1U24DK097215–01A1 (RCSIRM UKy) awarded to Y.Z. NMR spectra and IC-MS were recorded at the Center for Environmental Systems Biochemistry, University of Kentucky, supported in part by NCI, National Institutes of Health, Cancer Center Support Grant P30 CA177558.

The abbreviations used are:

UCP2	uncoupling protein 2
PFKFB2	6-phosphofructo-2-kinase/fructose-2,6-biphosphatase 2
glc-1-P	glucose-1-phosphate
gal-1-P	glactose-1-phosphate
α-KG	alpha-ketoglutarate
ALT	alanine amino transferase
OAA	oxaloacetic acid
Asp	Aspartate
GOT	glutamic-oxaloacetic transaminase
Glu	Glutamate
Gln	glutamine
IMP	inosine monophosphate

References

1. Hanahan D. Weinberg RA, Cell 2011, 144, 646. [PubMed: 21376230]
2. Warburg O, Biochem. Zeitschr 1923, 142, 317.
3. Koppenol WH, Bounds PL, Dang CV, Nat. Rev. Cancer 2011, 11, 325–337. [PubMed: 21508971]
4. Warburg O, Science 1956, 123, 309. [PubMed: 13298683]
5. Boroughs LK, DeBerardinis RJ, Nat. Cell Biol 2015, 17, 351. [PubMed: 25774832]
6. Guppy M, Leedman P, Zu X, Russell V, Biochem J. 2002, 364, 309. [PubMed: 11988105]
7. Bruntz RC, Lane AN, Higashi RM, Fan TW-M, J. Biol. Chem 2017, 292, 11601. [PubMed: 28592486]
8. Sellers K, Fox MP, Bousamra M, Slone S, Higashi RM, Miller DM, Wang Y, Yan J, Yuneva MO, Deshpande R, Lane AN, Fan TW, J. Clin. Invest 2015, 125, 687. [PubMed: 25607840]
9. Le A, Lane AN, Hamaker M, Bose S, Gouw A, Barbi J, Tsukamoto T, Rojas CJ, Slusher BS, Zhang H, Zimmerman LJ, Liebler DC, Slebos RJ, Lorkiewicz PK, Higashi RM, Fan TW, Dang CV, Cell Metab. 2012, 15, 110. [PubMed: 22225880]
10. Boroughs LK, DeBerardinis RJ, Nat. Cell Biol 2015, 17, 351. [PubMed: 25774832]
11. Sullivan LB, Gui DY, Hosios AM, Bush LN, Freinkman E, Vander Heiden MG, . Cell 2015, 162, 552. [PubMed: 26232225]
12. Hattori A, Tsunoda M, Konuma T, Kobayashi M, Nagy T, Glushka J, Tayyari F, McSkimming D, Kannan N, Tojo A, Edison AS, Ito T, Nature 2017, 545, 500. [PubMed: 28514443]
13. Possemato R, Marks KM, Shaul YD, Pacold ME, Kim D, Birsoy K, Sethumadhavan S, Woo HK, Jang HG, Jha AK, Chen WW, Barrett FG, Stransky N, Tsun ZY, Cowley GS, Barretina J, Kalaany NY, P Hsu P, Ottina K, Chan AM, Yuan B, Garraway LA, Root DE, Mino-Kenudson M, Brachtel EF, Driggers EM, Sabatini DM, Nature 2011, 476, 346. [PubMed: 21760589]
14. V Liberti M,. Locasale JW, Trends Biochem. Sci 2016, 41, 211. [PubMed: 26778478]
15. Ward PS, Thompson CB, Cancer Cell 2012, 21, 297. [PubMed: 22439925]
16. Zong WX, Rabinowitz JD, White E, Mol Cell 2016, 61, 667. [PubMed: 26942671]
17. Carew JS, Huang P, Mol. Cancer 2002, 1, 9. [PubMed: 12513701]
18. Brandon M, Baldi PA, Wallace DC, Oncogene 2006, 25, 4647. [PubMed: 16892079]
19. Baffy G, Mitochondrion 2010, 10, 243. [PubMed: 20005987]
20. Sreedhar A, Zhao Y, Mitochondrion 2017, 34, 135–140. [PubMed: 28351676]
21. Brand MD, Esteves TC, Cell Metab. 2005, 2, 85. [PubMed: 16098826]
22. Echtay KS, Murphy MP, Smith RA, Talbot DA, Brand MD, J. Biol. Chem 2002, 277, 47129. [PubMed: 12372827]
23. Li W, Nichols K, Nathan CA, Zhao Y, Cancer Biomark. 2013, 13, 377. [PubMed: 24440978]
24. Derdak Z, Mark NM, Beldi G, Robson SC, Wands JR, Baffy G, Cancer Res. 2008, 68, 2813. [PubMed: 18413749]
25. Sreedhar A, Lefort J, Petruska P, Gu X, Shi R, Miriyala S, Panchatcharam M, Zhao Y, Mol. Carcinog 2017, 56, 2290. [PubMed: 28574619]
26. Sreedhar A, Petruska P, Miriyala S, Panchatcharam M, Zhao Y, Oncotarget 2017, 8, 95504. [PubMed: 29221144]
27. Vozza A, Parisi G, De Leonardis F,Lasorsa FM, Castegna A, Amorese D, Marmo R, Calcagnile VM, Palmieri L, Ricquier D, Paradies E, Scarcia P, Palmieri F, Bouillaud F, Fiermonte G, Proc. Natl. Acad. Sci. U.S.A 2014, 111, 960. [PubMed: 24395786]
28. Bouillaud F, Biochim. Biophys. Acta 2009, 1787, 377. [PubMed: 19413946]
29. Lane AN, Fan TW-M, Higashi RM, Methods Cell Biol. 2008, 84, 541. [PubMed: 17964943]
30. Colburn NH, Bruegge WV, Bates JR, Gray RH, Rossen JD, Kelsey WH, Shimada T, Cancer Res. 1978, 38, 624. [PubMed: 626967]
31. Fan TW-M, Lane AN, Assignment strategies for NMR resonances in metabolomics research, in Methodologies for Metabolomics: Experimental Strategies and Techniques, Lutz N, Sweedler JV, Weevers RA, Editors. Cambridge University Press: Cambridge 2013.

32. Wishart DS, Jewison T, Guo AC, Wilson M, Knox C, Liu Y, Djoumbou Y, Mandal R, Aziat F, Dong E, Bouatra S, Sinelnikov I, Arndt D, Xia J, Liu P, Yallou F, Bjorndahl T, Perez-Pineiro R, Eisner R, Allen F, Neveu V, Greiner R, Scalbert A, Nucleic Acids Res. 2013, 41, D801. [PubMed: 23161693]

33. Fan TW, Warmoes MO, Sun Q, Song H, Turchan-Cholewo J, Martin JT, Mahan A, Higashi RM, Lane AN, Cold Spring Harb. Mol. Case Stud 2016, 2, a000893. [PubMed: 27551682]

34. Moseley HN, BMC Bioinform. 2010, 11, 139.

35. Lane AN, Fan TW-M, Xie Z, Moseley HN, Higashi RM, Anal. Chim. Acta 2009, 651, 201. [PubMed: 19782812]

36. Fan TW-M,Lane AN, Prog. Nucl. Magn. Reson. Spectrosc 2016, 92–93, 18.

37. Pecqueur C, Alves-Guerra C, Ricquier D, Bouillaud F, IUBMB life 2009, 61, 762. [PubMed: 19514063]

38. Fan TW, Lane AN, Higashi RM, Farag MA, Gao H, Bousamra M, Miller DM, Mol. Cancer 2009, 8, 41. [PubMed: 19558692]

39. Bridges RJ, Natale NR, Patel SA, Br. J. Pharmacol 2012, 165, 20. [PubMed: 21564084]

Significance of the Study:

UCP2 is a mitochondrial ion/anion transporter, and is known to regulate energy production. It is amplified in many human cancers, and it may directly or indirectly regulate cancer metabolism. However, there has been no systematic analysis of how UCP2 regulates cellular metabolism. To our knowledge, this is the first study to illustrate the metabolic changes caused by UCP2 upregulation using a stable isotope resolved metabolomics approach. The identified metabolites and metabolic enzymes may serve as potential biomarkers or therapeutic targets for UCP2 amplified cancers.

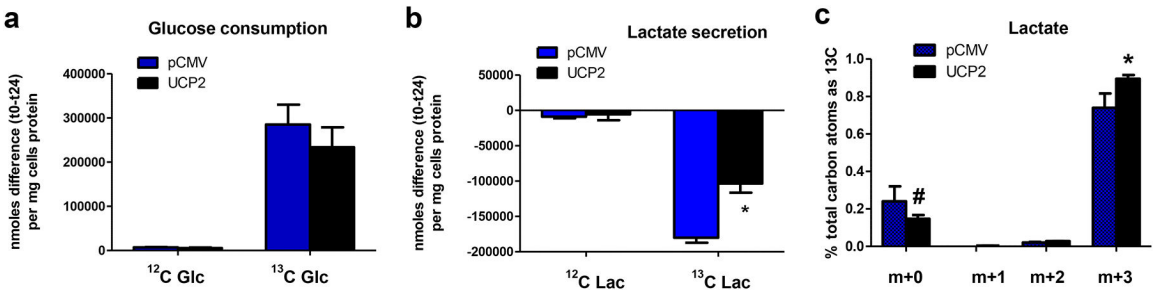

Figure 1. The dual metabolic nature of UCP2 overexpressing cells

^{13}C-glucose consumption (**a**) and lactate secretion into the medium (**b**) were measured by 1D ^{1}H NMR as described in the text. The metabolite amounts are expressed as nmoles/mg protein. **c**, Fractional isotopologue distributions of ^{13}C-lactate in cell extracts of control pCMV and UCP2 overexpressing cells. N= 4 per group. *, $p < 0.01$ and #, $p<0.05$. The error bars represent standard deviation (SD).

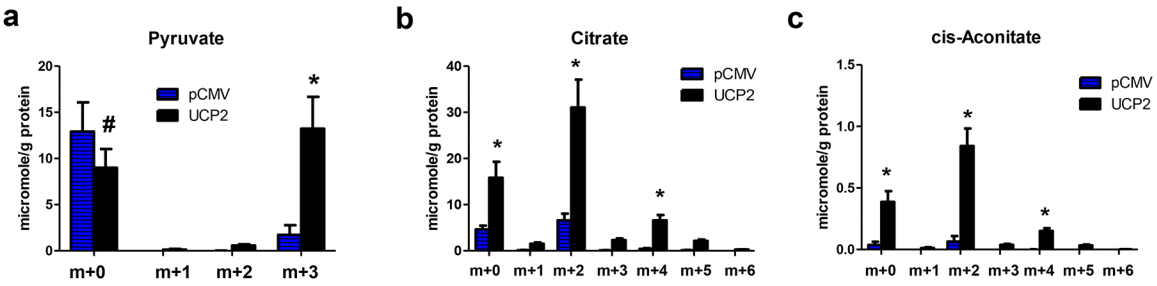

Figure 2. UCP2 overexpression increased ^{13}C labeling in pyruvate

a, Isotopologue concentration of ^{13}C-pyruvate in cell extracts of control pCMV and UCP2 overexpressing cells showing increased labeled incorporation in UCP2 overexpressing cells. Isotopologue abundances were determined from IC-FTMS. The incorporation of ^{13}C atoms from ^{13}C-Glc into (m-2, m-4) citrate (**b)** and cis-aconitate (**c**). N= 4 per group. *, $p<0.01$ and #, $p<0.05$. The error bars represent standard deviation (SD).

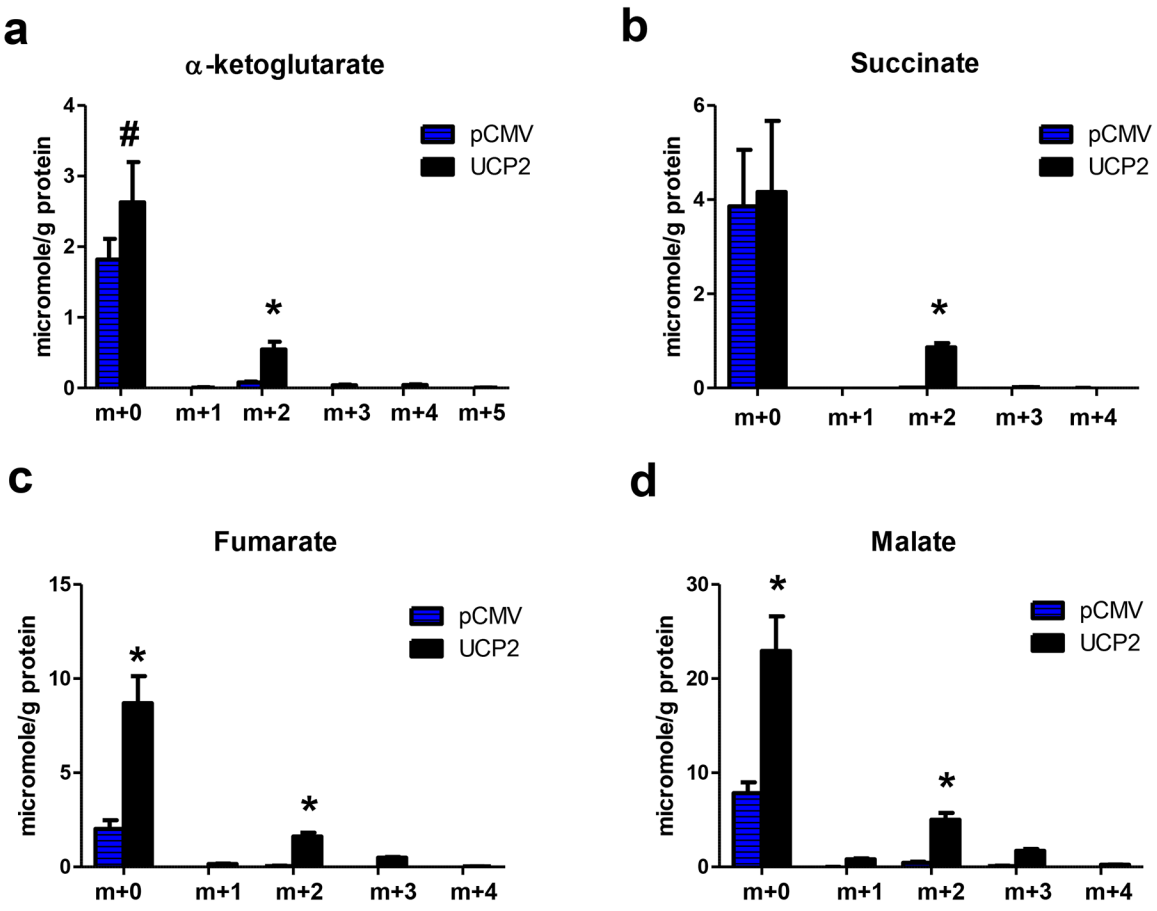

Figure 3. Increased pyruvate oxidation and TCA cycle flux in UCP2 overexpressing cells

The incorporation of ^{13}C atoms from ^{13}C-Glc into (m+2) α-ketoglutarate (**a**), succinate (**b**), fumarate (**c**), and malate (**d**) were determined by IC-FTMS. N = 4 per group. *, $p<0.01$, #, $p<0.05$. The error bars represent standard error deviation (SD).

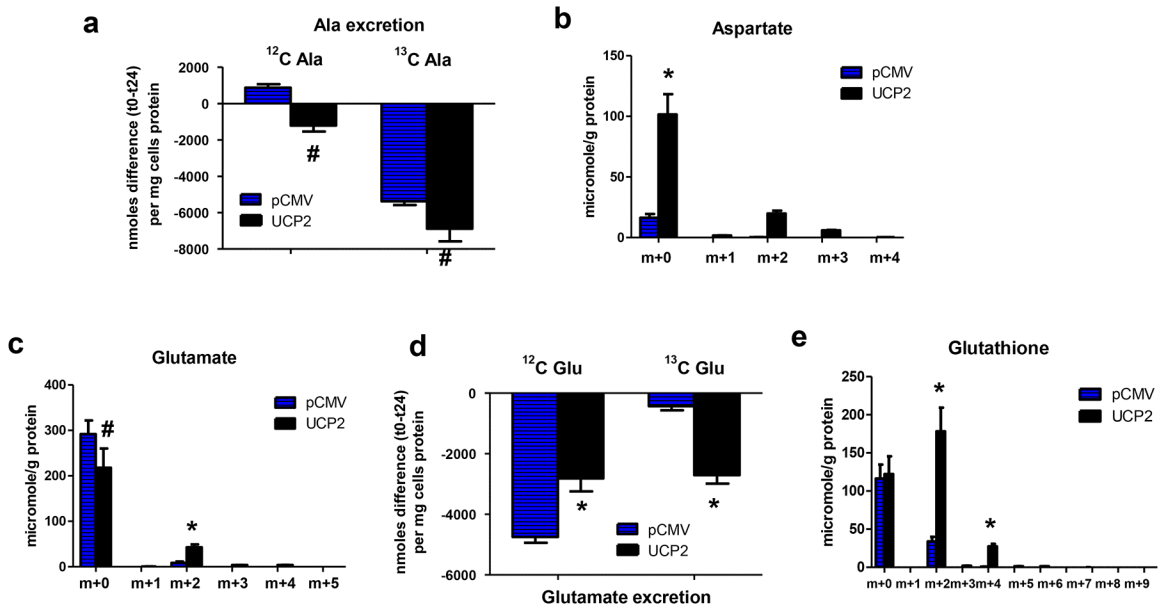

Figure 4. Increased *de novo* amino acid synthesis in UCP2 overexpressing cells

^{13}C enrichment of alanine in the medium as determined by ^{1}H NMR (**a**). Concentrations of aspartate (**b**) and glutamate (**c**) in cell extracts of pCMV and UCP2 overexpressing cells were determined by IC-MS as described in the text. ^{13}C enrichment of glutamate in the medium (**d**). ^{13}C isotopologues of GSH in control pCMV and UCP2 overexpressing cells (**e**). N = 4 per group. *, $p<0.01$, #, $p<0.05$. The error bars represent standard deviation (SD).

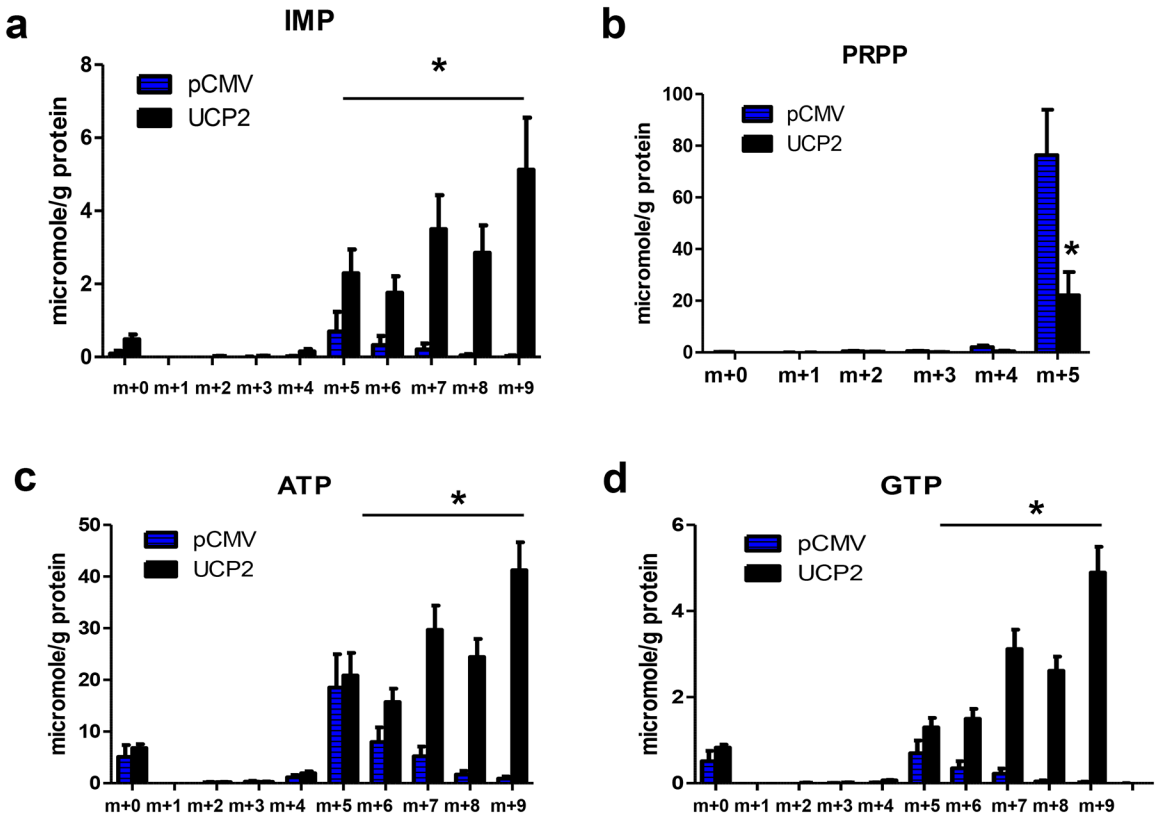

Figure 5. Significant enrichment of *de novo* purine biosynthesis

Purine nucleotide biosynthesis including inosine (**a**), PRPP (**b**), adenosine (**c**), and guanosine (**d**) was measured in control pCMV and UCP2 overexpressing cells by IC-FTMS. N = 4 per group. *, $p<0.01$. The error bars represent standard deviation (SD).

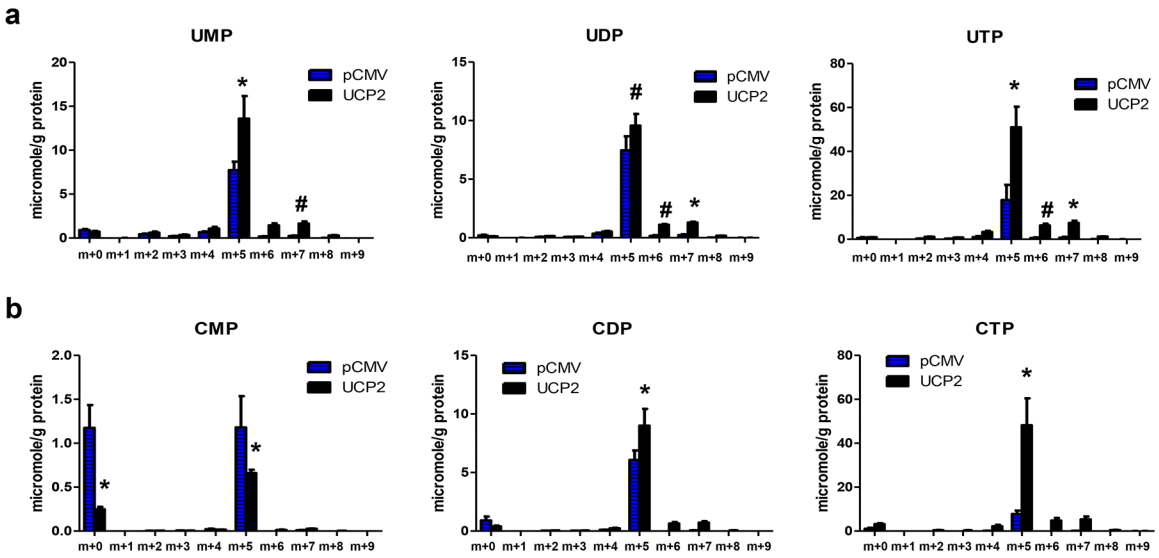

Figure 6. Mild enrichment of *de novo* pyrimidine biosynthesis

Pyrimidine biosynthesis including uridine (**a**) and cytidine (**b**) was measured in control pCMV and UCP2 overexpressing cells. N = 4 per group. *, $p<0.01$, #, $p<0.05$. The error bars represent standard deviation (SD).